

Oxygen diffusion behaviour in poly(ether urethane) cationomers based on 4,4'-methylenediphenyl isocyanate

Show-An Chen* and Wu-Chung Chan

Chemical Engineering Department, National Tsing-Hua University, Hsinchu, Taiwan 30043, China

(Received 6 November 1989; revised 31 March 1990; accepted 6 April 1990)

Dynamic oxygen permeation measurements are carried out on films cast from solutions and emulsions of polyurethane (PU) cationomers. For the former, ionization leads to the permeation coefficients P at 20–40°C (below the glass transition temperature of the hard domains, T_{gh}) being higher than those at 50–70°C (above T_{gh}) by a factor of about 10^2 . This is opposite to the results observed for normal homopolymers and un-ionized PU. For the latter, dispersion leads to a drop in P at 20–40°C and an increase in P at 50–70°C. These variations in P correlate quite well with the variation in morphology resulting from ionization and dispersion.

(Keywords: polyurethane; cationomers; oxygen diffusion; 4,4'-methylenediphenyl isocyanate)

INTRODUCTION

Studies on the permeation of simple gases through homopolymer films are extensive¹ and rather fundamental². However, those through block copolymer films such as poly(ether/ester urethane) (PU) and styrene-butadiene-styrene (SBS) are scarce. These two block copolymers have a discontinuity zone in the Arrhenius plot of the diffusion coefficient D at the onset of the glass transition of the hard domains^{3,4}. This phenomenon was attributed to the fact that, at temperatures higher than the glass transition temperature of the hard domains, T_{gh} , the gas molecules can diffuse not only through the soft domains but also through the hard domains³. For PU/polyepoxide interpenetrating networks at temperatures near T_{gh} , one of us⁵ found that there is a period of zero permeation rate before a steady permeation rate is reached during gas permeation measurements.

This work reports the effects of ionization and phase inversion on the diffusion behaviour and solubility of oxygen in PU cationomers.

EXPERIMENTAL

Descriptions of the chemicals used and procedures for preparation and emulsification of the PU cationomer with poly(tetramethylene oxide) (PTMO) of molecular weight 2000 as soft segment, 2,2'-methyliminodiethanol (MIDE) as chain extender, glycolic acid as quaternization agent and 4,4'-methylenediphenyl isocyanate (MDI) as diisocyanate were given in the preceding work⁶. The reaction procedure can be summarized as in *Scheme 1*.

Samples were also designated in the same way: for example, M-1-6-5-1.0-20°C means 1 mol of PTMO, 6 mol of MDI, 5 mol of MIDE and 1.0 mol ratio of glycolic acid to MIDE are used and the dispersion

temperature is 20°C; the first letter 'M' refers to MDI. The three samples, M-1-6-5-0, M-1-6-5-1.0 and M-1-6-5-1.0-20°C, were cast into films of 0.05–0.15 mm thickness at room temperature.

A Hitachi H-600 transmission electron microscope (TEM) operating at 75 kV with magnification of 20 000× was used to examine the morphology of the samples. Microtomed specimens were directly mounted on 400-mesh copper grids without a supporting film. They were then stained with OsO₄ by a well developed technique⁷ applicable for polyurethanes⁸. During TEM observation, special precautions were taken to minimize electron beam damage to the specimens by focusing on an area and translating to an adjacent area for recording.

Oxygen permeations through the films were measured using the high-vacuum technique developed by Barrer⁹. The penetrant was made to flow over one side of the film; the cumulative amount of gas that has passed through the film is detected by use of a mercury manometer to measure the pressure increase in the constant-volume receiving chamber. The oxygen permeation coefficient P was calculated using the equation:

$$P = V_r l / A \Delta p$$

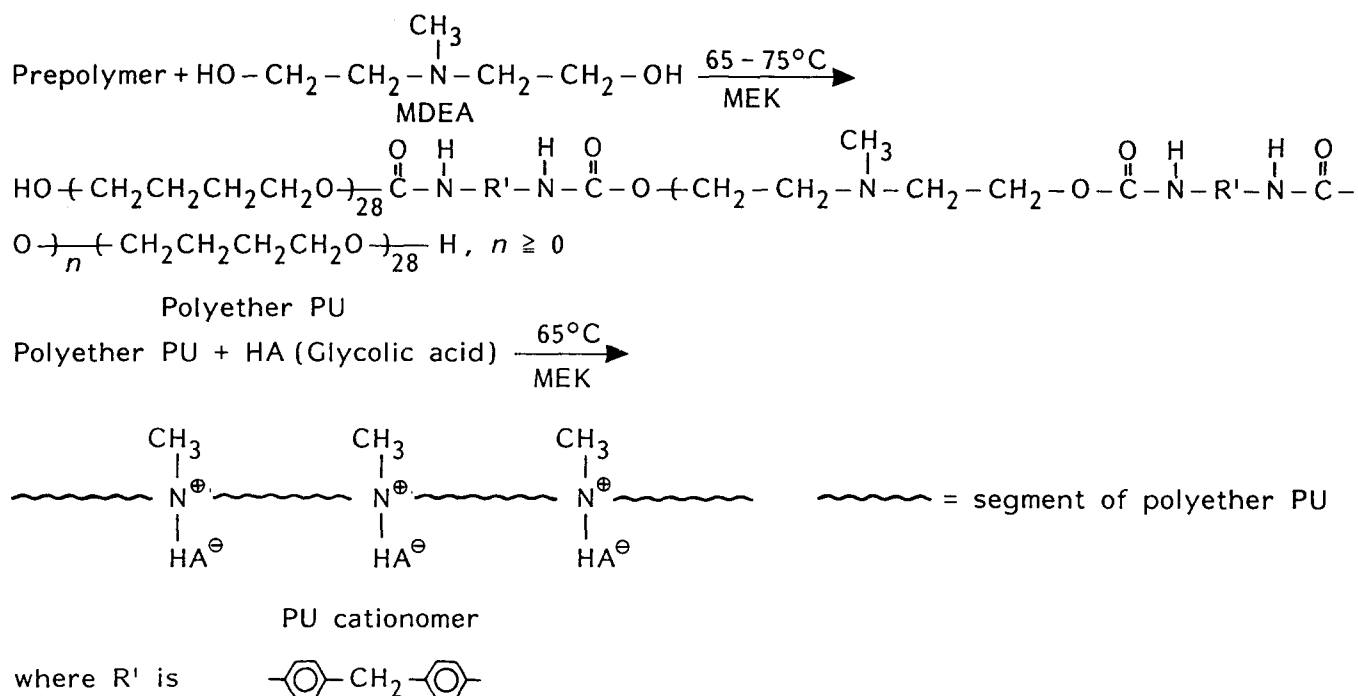
where V_r is the volume of gas permeated (based on STP) per second at steady state, l is the film thickness (cm), A is the film cross-sectional area for gas permeation (cm²) and Δp is pressure drop (equal to 76 cmHg). The diffusion coefficient D was calculated from data for total permeation Q_t versus time using Barrer's time lag method⁹:

$$D = l^2 / 6\theta$$

where θ is the time at which the extrapolated linear portion of the Q_t curve (steady-state portion) intersects the time axis. The solubility coefficient S of oxygen in the film was then calculated using the relation:

$$P = DS$$

* To whom correspondence should be addressed



Scheme 1

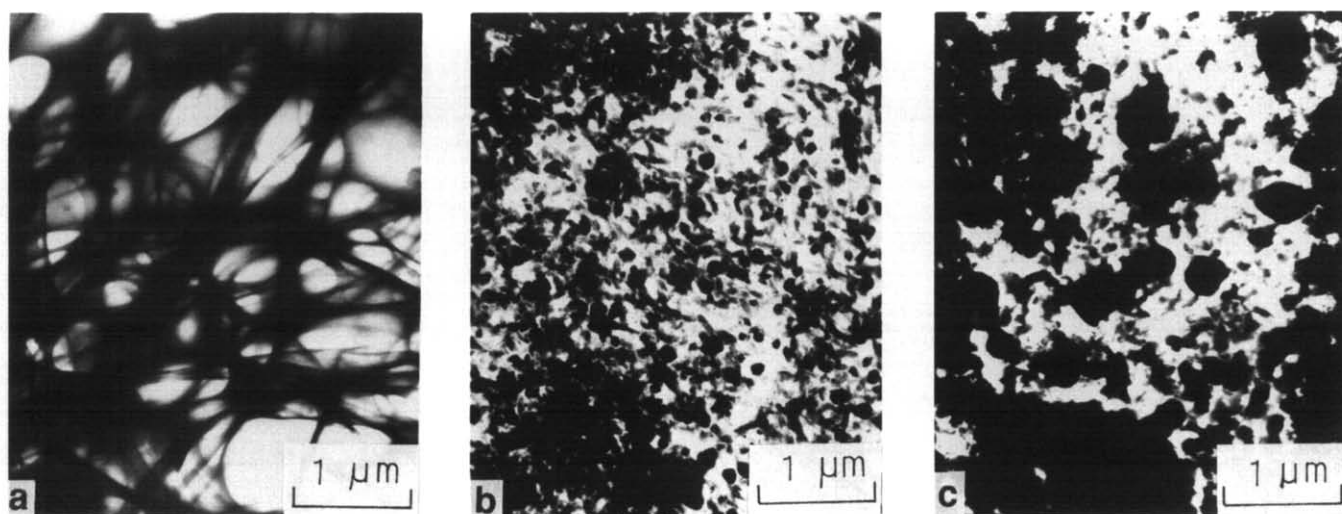


Figure 1 The TEM micrographs of the MDI series materials: (a) M-1-6-5-0, (b) M-1-6-5-1.0, (c) M-1-6-5-1.0-20°C

The activation energies and pre-exponential factors of oxygen permeation and diffusion were calculated using the Arrhenius expressions:

$$P = P_0 \exp(-E_p/RT)$$

and

$$D = D_0 \exp(-E_d/RT)$$

The heat of solution H_s was calculated from the equation¹⁰:

$$H_s = E_p - E_d$$

or alternatively from the relation¹¹:

$$H_s = -R d \ln S/d(1/T)$$

The pre-exponential factor D_0 from the Eyring rate theory is expressed as:

$$D_0 = (e\lambda^2kt/h) \exp(\Delta S^*/R)$$

where λ is the jump length of a diffusing molecule and ΔS^* the entropy of activation for diffusion.

RESULTS AND DISCUSSION

Morphological changes after dispersion with water

The TEM micrographs of the MDI films cast from solutions (M-1-6-5-0 and M-1-6-5-1.0) and emulsion (M-1-6-5-1.0-20°C) are shown in Figure 1. The M-1-6-5-0 sample (Figure 1a) shows a morphology with soft domains as the continuous phase and hard domains as a fibrillar network penetrating the continuous phase. Upon ionization (M-1-6-5-1.0), owing to decreased order and increased cohesion in the hard domains⁶, the hard domains lose their fibrillar network characteristic and aggregate to form globules and agglomerates dispersed in the continuous phase (Figure 1b). After dispersion at 20°C (which is 35°C lower than the glass transition

temperature of the hard domains⁶, $T_{gh} = 55^\circ\text{C}$), owing to difficulty in segmental motion in the hard domains, water can only penetrate into parts of the ordered hard domains⁶. Thus partial phase inversion occurs and some of the hard segments are exposed on the particle surface in the emulsion. During film formation, the particles coagulate to form a film with the morphology having interweaving soft and hard domains (Figure 1c).

Oxygen diffusion behaviour

Dynamic oxygen permeation curves (total permeation versus time) of the un-ionized PU (M-1-6-5-0), the ionized PU (M-1-6-5-1.0) and the dispersed PU at 20°C (M-1-6-5-1.0- 20°C) are shown in Figures 2–4. The permeability P , diffusion coefficient D and solubility coefficient S calculated from the steady permeation data at various temperatures from 20 to 70°C are plotted versus $1/T$ and are shown in Figures 5–7. The characteristic values of the temperature plots (activation energies, pre-exponential factors and heats of solution) are listed in Table 1.

Before ionization (M-1-6-5-0), the permeation rate from 20 to 40°C (well above the glass transition

temperature of the soft domains, T_{gs} , and below the glass transition temperature of the hard domains, T_{gh}) increases gradually to the steady rate as in the case of a polymer in the rubbery state (Figure 2), and thus the diffusion is Fickian. In addition, the hard domains are fibrillar-network-like penetrating the continuous phase (soft domains) (Figure 1a). Thus, oxygen would mainly permeate through the continuous phase in this temperature range. As the temperature increases to a higher level, from 50 to 70°C ($T \geq T_{gh}$), the permeation rate is higher initially, then decreases and subsequently increases to reach the steady rate. This rate variation is similar to that in vapour sorption of a polymer at its glass transition temperature due to sudden surface swelling, which generates stress and molecular relaxation effects¹². However, the solubility of a gas in a polymer is much smaller than that of an organic vapour; such stress generation and relaxation will never occur. An explanation for this rapid initial permeation rate is outlined below. Since, in the T_{gh} region, parts of the hard segments are able to rotate and the other parts are still frozen, some microvoids could be generated in the hard domains¹³, allowing neighbouring oxygen molecules to be accommodated without waiting for the creation of new holes. Initially the microvoids are empty, allowing the diffusing oxygen molecules to be accommodated. Part

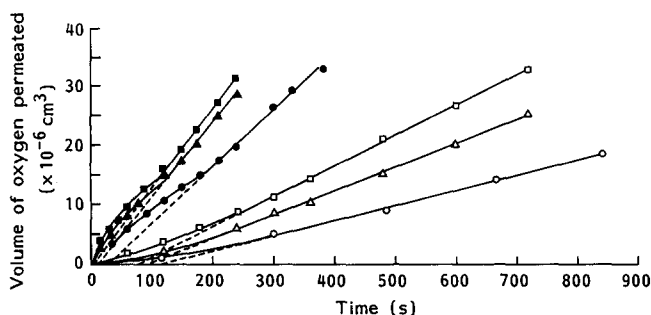


Figure 2 Dynamic oxygen permeation curves of M-1-6-5-0 material at various temperatures: (○) 20°C , (△) 30°C , (□) 40°C , (●) 50°C , (▲) 60°C , (■) 70°C

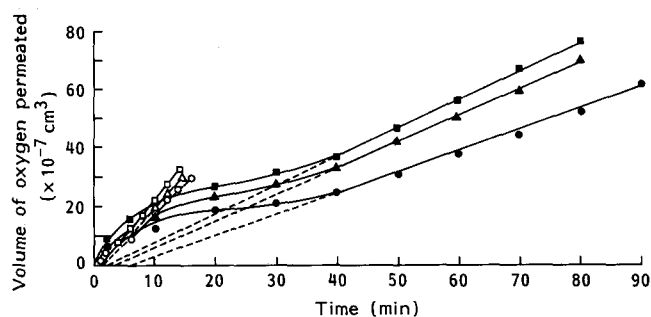


Figure 3 Dynamic oxygen permeation curves of M-1-6-5-1.0 material at various temperatures: (○) 20°C , (△) 30°C , (□) 40°C , (●) 50°C , (▲) 60°C , (■) 70°C

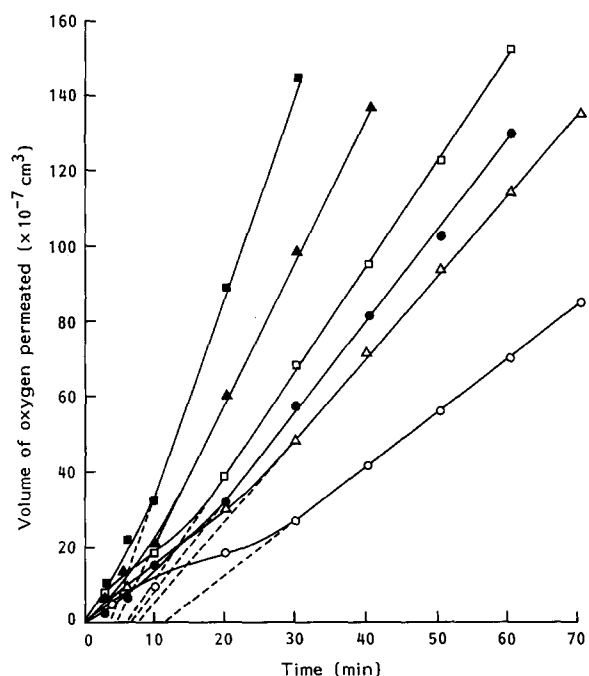


Figure 4 Dynamic oxygen permeation curves of M-1-6-5-1.0- 20°C material at various temperatures: (○) 20°C , (△) 30°C , (□) 40°C , (●) 50°C , (▲) 60°C , (■) 70°C

Table 1 The activation energy, pre-exponential factor and heat of solution of oxygen diffusion and permeation of the MDI system^a

Sample	E_d (kcal mol ⁻¹)		D_0 (10^{-5} cm ² s ⁻¹)		E_p (kcal mol ⁻¹)		P_0 (10^{-5} cm ³ cm cm ⁻² s ⁻¹ cmHg ⁻¹)		H_s (kcal mol ⁻¹)	
	Low T	High T	Low T	High T	Low T	High T	Low T	High T	Low T	High T
M-1-6-5-0	3.30	10.75	9.64	2626000	6.56	5.70	199	61.5	3.26	-5.05
M-1-6-5-1.0	0.93	9.34	0.078	12000	2.35	2.58	0.191	0.0069	1.42	-6.76
M-1-6-5-1.0- 20°C	5.68	7.15	21.3	150	6.26	9.14	11.4	628	0.58	0.58

^aLow T and High T mean the low-temperature range, 20 – 40°C , and high-temperature range, 50 – 70°C

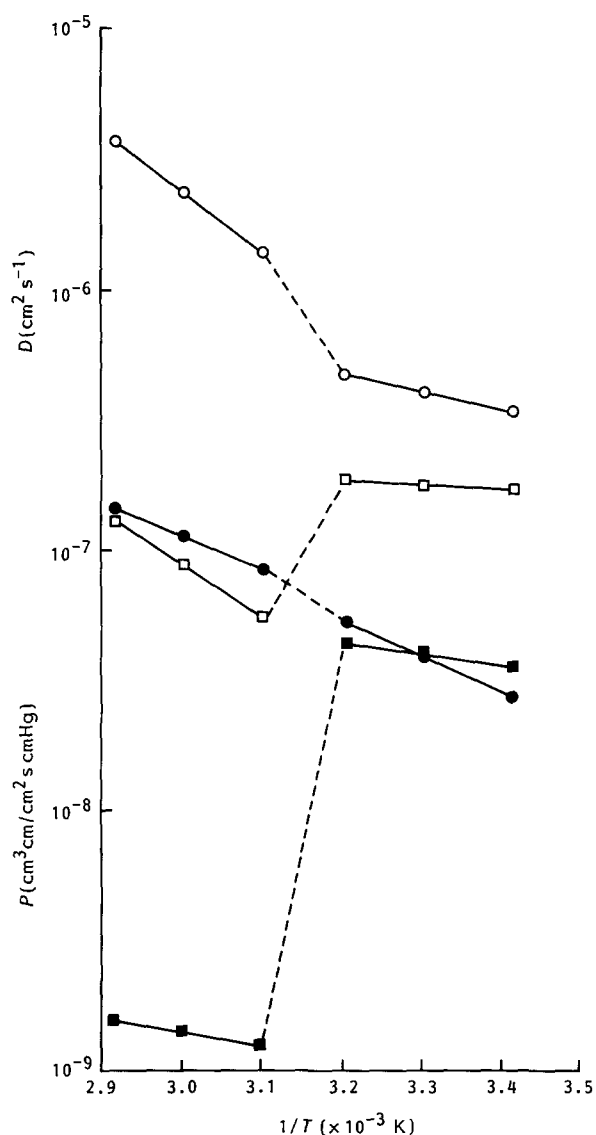


Figure 5 Permeability (●, ■) and diffusion (○, □) coefficients versus $1/T$ of the M-1-6-5 series materials: (○, ●) M-1-6-5-0, (□, ■) M-1-6-5-1.0

of these oxygen molecules could diffuse through the film via parts of the disordered fibrillar network of hard domains having microvoids, while the other part of these oxygen molecules in the hard domains could diffuse into the soft domains. Thus the observed initial permeation rate is higher. As the permeation proceeds further, parts of the microvoids are occupied, and the local permeation rate through the hard domains slows down. As the steady state is reached, the fraction of microvoids occupied by oxygen also reaches a steady value and the fraction of diffusing oxygen molecules not diffusing into the disordered hard domains increases to a steady value. The oxygen molecules passing through both soft and hard domains have thus increased their path length compared to those passing through soft domains only. The change of heat of solution H_s from positive at lower temperature ($T_{gs} < T < T_{gh}$) to negative at higher temperature ($T \geq T_{gh}$) also supports this interpretation, as illustrated below.

The heat of solution H_s is the sum of the work required to create a hole to accommodate the solute molecule (an endothermic process) and the interaction energy between

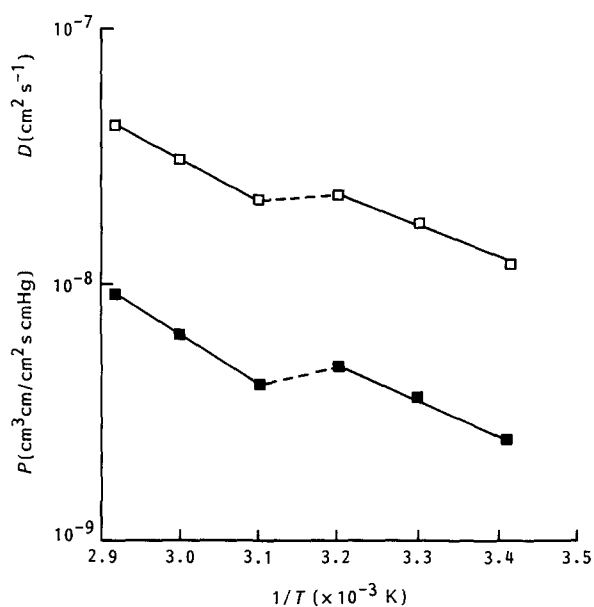


Figure 6 Permeability (■) and diffusion (□) coefficients versus $1/T$ of M-1-6-5-1.0-20°C material

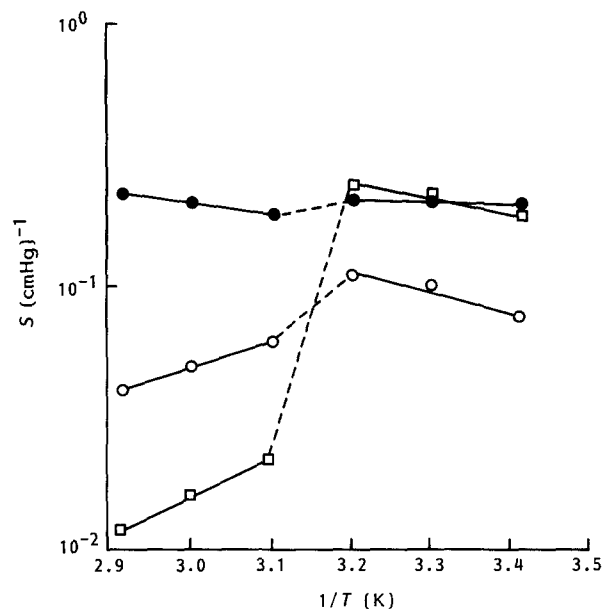


Figure 7 Solubility coefficient versus $1/T$ of the M-1-6-5 series materials: (○) M-1-6-5-0, (□) M-1-6-5-1.0, (●) M-1-6-5-1.0-20°C

this molecule and the surrounding chain segments in the original position (an exothermic process)^{2,11}. Before ionization, as $T_{gs} < T < T_{gh}$, H_s is positive (Table 1), implying that the former is predominant and oxygen molecules diffuse mainly through the soft domains. As $T \geq T_{gh}$ (Table 1), H_s is negative, implying that the latter is predominant and there are holes available in the hard domains into which oxygen molecules may jump.

The activation energy for diffusion E_d is governed by the energy required to separate the segments surrounding the diffusing molecules to give a space of sufficient cross section for them to pass¹¹. The E_d at 20–40°C is lower than that at 50–70°C (Table 1), indicating that diffusing oxygen molecules also pass through the hard domains at 50–70°C. The pre-exponential factor D_0 at 20–40°C is much smaller than that at 50–70°C, which further

supports the consideration that diffusing oxygen molecules also pass through the hard domains at higher temperatures. The reason is that D_0 increases with the entropy of activation ΔS^* , which reflects the disturbance of the surrounding segments so as to free the gas molecules¹¹, and ΔS^* for oxygen molecules in the hard domains would be much larger than that in the soft domains, as is the case. Since both permeability P and diffusion coefficient D increase with T without an abrupt change in the entire temperature range, the fraction of oxygen molecules that diffuses through the hard domains would be small.

After ionization (M-1-6-5-1.0), variations of permeability P , diffusion coefficient D and solubility coefficient S versus $1/T$ show sudden drops at 50°C; at lower temperature P and D are higher than those at higher temperature, opposite to that of homopolymers. Such drops are mainly due to morphological change, as illustrated below. At 20–40°C, oxygen mainly diffuses through the continuous phase (the soft domains). As the temperature rises to 50–70°C, some oxygen molecules in the soft domains also diffuse into the hard domains, as reflected in the changing permeation rate from the rapid initial value to the very slow rate, before reaching the steady rate. In addition, as $T \geq T_{gh}$, the value of heat of solution H_s turns from positive to negative and is lower than that for the un-ionized case, indicating that more holes are available after ionization. This fact also provides evidence. Since the hard domains form globules and agglomerates dispersed in the continuous phase, at the higher temperature level, those oxygen molecules diffusing into the dispersed hard domains must pass through the soft domains before permeating through the film. Thus the diffusion path length increases to a much higher extent than that before ionization (in which the hard domains form fibrillar-like networks) due to an increase in the temperature. Thus, at higher temperature, D drops significantly after ionization, and P also drops to a much higher extent due to additional decrease in S after ionization.

After dispersion (M-1-6-5-1.0-20°C), at the lower temperature level (20–40°C), permeability P and diffusion coefficient D drop significantly more than those before dispersion and ionization. But at higher tempera-

ture (50–70°C), P is located between and D is lower than those before dispersion and ionization. These changes can also be explained by the variation in morphology after dispersion.

After dispersion, the hard and soft domains are interwoven (Figure 1c), and order in the hard domains is further disrupted⁶. The film surface area occupied by the soft domains is much less than that before dispersion. At the lower temperature level, oxygen molecules mainly permeate through the soft domains; thus both permeability P and diffusion coefficient D should drop after dispersion. At the higher temperature level, oxygen can also permeate simultaneously through the hard domains, but at a lower rate than through the soft domains. Thus D should be lower than that before dispersion. However, at higher temperature, P increases after dispersion, resulting from the high solubility coefficient S . This high S could be due to the increased disorder in the hard domains.

ACKNOWLEDGEMENT

The authors wish to thank the National Science Council of the Republic of China for financial aid.

REFERENCES

- 1 Crank, J. and Park, G. S. 'Diffusion in Polymers', Academic Press, New York, 1968
- 2 Meares, P. *J. Am. Chem. Soc.* 1954, **76**, 3415
- 3 McBride, J. S., Massaro, T. A. and Cooper, S. L. *J. Appl. Polym. Sci.* 1979, **23**, 201
- 4 Odani, H., Taira, K., Nemoto, N. and Kurada, M. *Bull. Inst. Res. Kyoto Univ.* 1975, **53**, 216
- 5 Chen, S. A. and Ju, H. L. *J. Appl. Polym. Sci.* 1980, **25**, 1105
- 6 Chen, S. A. and Chan, W. C. *Makromol. Chem.* 1988, **189**, 1523
- 7 Wegner, G., Zhu, L. L. and Lieser, G. *Makromol. Chem.* 1981, **182**, 231
- 8 Chan, K. W. and Geil, P. H. *Polymer* 1983, **26**, 490
- 9 Barrer, R. M. *Trans. Faraday Soc.* 1939, **35**, 628
- 10 Michaels, A. and Bixler, H. J. *J. Polym. Sci.* 1961, 413
- 11 Meares, P. 'Polymers: Structure and Bulk Properties', Van Nostrand, London, 1965, pp. 321–6
- 12 Kishimoto, A., Fujita, H., Odani, H., Kurata, M. and Tamura, M. *J. Phys. Chem.* 1960, **64**, 594
- 13 Meares, P. 'Polymers: Structure and Bulk Properties', Van Nostrand, London, 1965, p. 270